Extended Abstracts of the 1996 International Conference on Solid State Devices and Materials, Yokohama, 1996, pp. 691-693

Tunneling Spectroscopy of InAs Wetting Layers and Coherent Islands: Resonant Tunneling through Two- and Zero-Dimensional Electronic States

T. Suzuki,* K. Nomoto, K. Taira, and I. Hase
Sony Corporation Research Center,
174 Fujitsuka-cho, Hodogaya-ku, Yokohama, 240, JAPAN

We have investigated the tunneling current through InAs wetting layers and coherent islands using GaAs/AlGaAs/InAs/AlGaAs/GaAs tunneling diodes. For the diodes both with and without the coherent islands, tunneling current through two-dimensional electronic states in the wetting layers is observed. On the other hand, additional fine structure in the current-voltage characteristics due to resonant tunneling through zero-dimensional electronic states in the coherent islands and Coulomb blockade effects are observed only for the case of an InAs layer with the coherent islands.

1 Introduction

The Stranski-Krastanow (SK) growth mode for lattice mismatched semiconductors, such as Ge on Si[1)], In(Ga)As on GaAs[2-8)], leads to the self-organized formation of coherent islands (quantum dots) after growth of the wetting layer. The fabrication methods making use of this growth mode are considered to be promising methods of fabricating quantum dots because they do not need nanolithography. By means of photoluminescence (PL) and cathodoluminescence (CL), the optical properties of the coherent islands have been studied extensively[3,9-12)]. Although a PL peak for an ensemble of many islands has a full width at half maximum of several tens of meV due to the size deviation of the islands, for the case of a small number of the islands, extremely sharp luminescence peaks due to the δ function-like zero-dimensional electron and hole density of states of the individual islands have been clearly confirmed[11,12)]. On the other hand, although the ensemble of energy levels of electrons and holes in the islands has been investigated by means of capacitance spectroscopy[13,14)], little attempt to study the electronic properties of the coherent islands has been made. In order to study tunneling phenomena through the coherent islands, we have fabricated GaAs/AlGaAs/InAs/AlGaAs/GaAs tunneling diode structures, in which an ultra-thin InAs layer with/without coherent islands is embedded in AlGaAs barriers, and performed tunneling current spectroscopy. As a result, we have observed tunneling phenomena through two-dimensional (2D) electronic states in the InAs wetting layer for the tunneling diodes both with and without the coherent islands, and zero-dimensional (0D) electronic states in the InAs coherent islands only for the tunneling diodes with the coherent islands. Moreover, we have observed Coulomb blockade phenomena in the tunneling diodes with the coherent islands. The corresponding capacitance value is consistent with the lateral size of the coherent islands obtained from atomic force microscope (AFM) measurement.

2 Sample structures

The diodes used in this study were grown by molecular beam epitaxy (MBE) on (001)-oriented 1×10^{18} cm^{-3} Si-doped n-GaAs substrates. The grown heterostructures

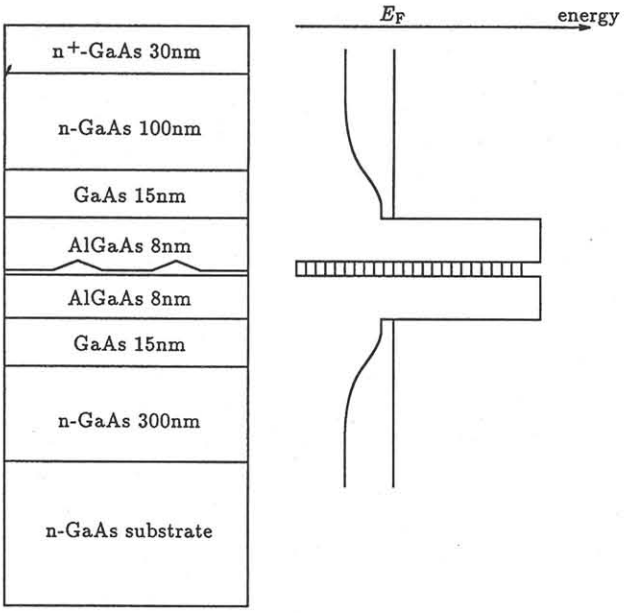

Figure 1: Layer structure of the diodes used in this study and a schematic conduction band profile.

are as follows: (i)n-GaAs bottom contact layer (300 nm, $n = 5 \times 10^{17}$ cm^{-3}), (ii)GaAs spacer layer (15 nm), (iii)$Al_{0.24}Ga_{0.76}As$ bottom barrier (8 nm), (iv)InAs layer (sample A: 1.8 monolayers, sample B: 1.4 monolayers, and sample C: 1.0 monolayers), (v)$Al_{0.24}Ga_{0.76}As$ top barrier (8 nm), (vi)GaAs spacer layer (15 nm), (vii)n-GaAs layer (100 nm, $n = 5 \times 10^{17}$ cm^{-3}), and (viii)n$^+$-GaAs top contact layer (30 nm, $n = 2 \times 10^{18}$ cm^{-3}) (Figure 1 shows the layer structure and a schematic conduction band profile). Silicon was used as the donor for the n-type layer. In order to avoid diffusion or segregation of silicon to the active region (AlGaAs/InAs/AlGaAs), sufficiently thick spacer layers are employed. The growth of InAs on AlGaAs proceeds via the SK mode. After two-dimensional growth of about 1.5 monolayers (ML) (growth of the wetting layer), the SK transition takes place leading to three-dimensional growth (spontaneous formation of the coherent islands) as confirmed by *in-situ* refractive high energy electron diffraction (RHEED) observations (the RHEED pattern changes from a streaky one to a spotty one). An AFM study of reference samples confirmed that, in the case of

*Electronic mail: tsuzuki@src.sony.co.jp

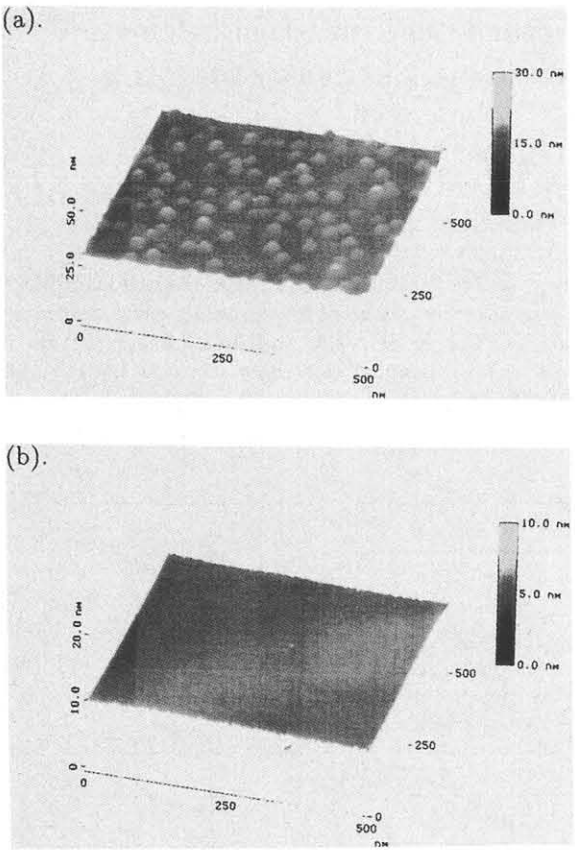

Figure 2: Surface AFM images of (a)1.8 ML InAs on AlGaAs, and (b)AlGaAs embedding the InAs layer.

sample A, coherent islands with height $\sim$ 4 nm, diameter $\sim$ 25 nm are spontaneously formed on the wetting layer with a number density of $\sim 4\times10^{10}$ cm^{-2}, but for samples B and C, the InAs layer consists of only the wetting layer. Figures 2(a) and (b) are surface AFM images of 1.8 ML InAs on AlGaAs and AlGaAs embedding the InAs layer, respectively. Although coherent islands are observed in Fig. 2(a), a smooth surface is shown in Fig. 2(b) suggesting that the desired diode structures were obtained. By means of conventional photolithography and dry etching, diode pillars with diameters of 1μm were defined. Therefore, the number of the coherent islands contained in a diode for sample A is several hundred.

3 *I-V* characteristics

Figure 3 shows current-voltage (*I-V*) and differential conductance-voltage (*G-V*) characteristics measured at 4.2 K in which the substrate contact is grounded. At $V \sim \pm$600-900 mV, structures, which are attributed to resonant tunneling (RT) from 3D states in the emitter to 2D states in the wetting layer, can be found. The onset of the 3D-2D RT is at a bias such that the Fermi energy of the emitter (E_{fe}) lines up with the 2D ground states in the wetting layer (E_{2g}), and the RT current increases with increase in the bias voltage beyond the onset. At a bias such that the bottom of conduction band of the emitter (E_{ce}) coincides with E_{2g}, the 3D-2D RT terminates and the RT current disappears quite abruptly. Al-

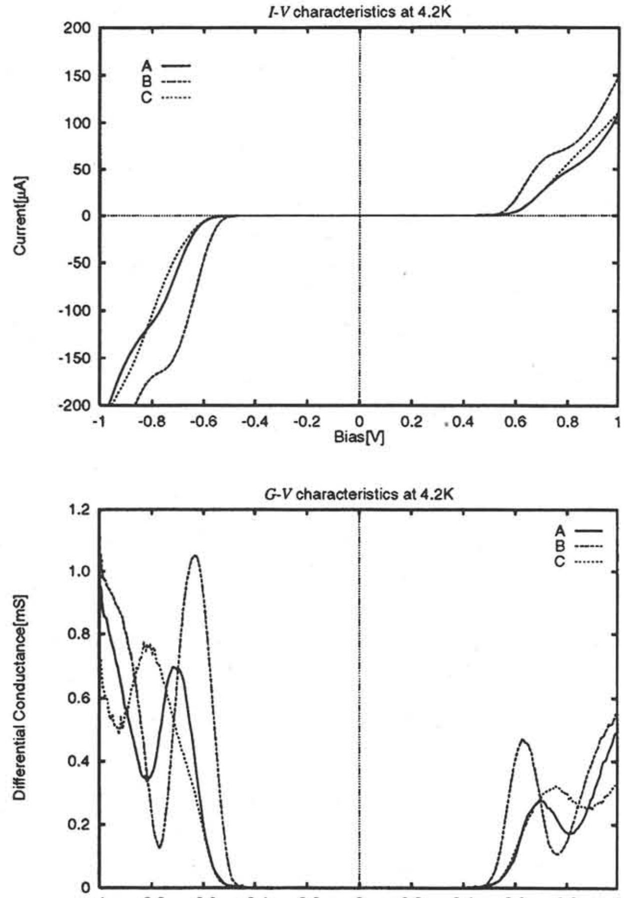

Figure 3: *I-V* and *G-V* characteristics of 1 μm diameter diodes measured at 4.2 K.

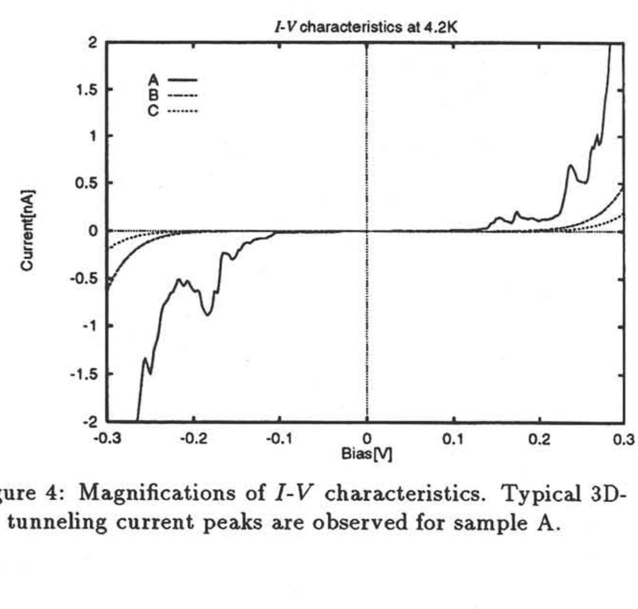

Figure 4: Magnifications of *I-V* characteristics. Typical 3D-0D tunneling current peaks are observed for sample A.

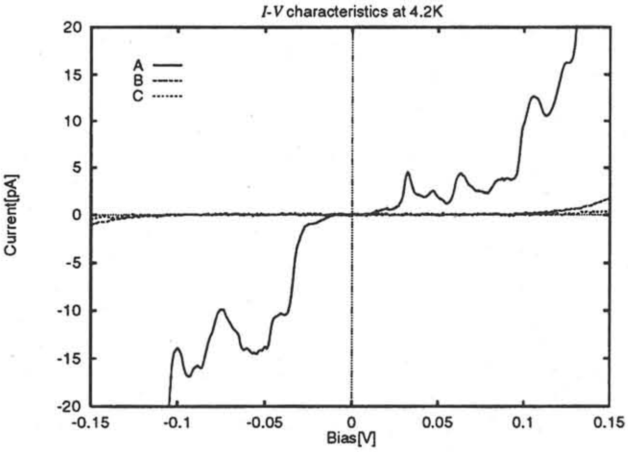

Figure 5: Low bias I-V characteristics. Near the origin, Coulomb blockade is observed.

though a clear negative differential resistance cannot be seen in our data due to a large direct tunneling current (from the emitter to the collector) in the rather high bias region, it was observed that the 3D-2D tunneling terminates at ±810 mV, ±760 mV, and ±880 mV, for sample A, B, and C, respectively. Comparing these data and a numerical calculation of band bending using the Poisson equation, we can conclude that $E_{2g} \sim 147$ meV, 140 meV, and 158 meV measured from the bottom of the GaAs conduction band, for sample A, B, and C, respectively.

In Fig. 4, which are magnifications of I-V characteristics of Fig. 3, we can observe additional peaks in the case of sample A, but not for samples B and C. Due to the fact that these peaks are obtained for only sample A, we consider that they are due to the RT from 3D states in the emitter to 0D states in the coherent islands. Since the ground state energy levels of the coherent islands are lower than the Fermi energy of the GaAs emitter/collector in the zero bias condition, as confirmed by our PL measurement, the observed 0D states are excited states in the coherent islands. In the case of 3D-0D RT, at the bias such that E_{fe} coincides with a 0D energy level in a coherent island (E_0), the onset of 3D-0D RT and a sharp rise in the RT current should be observed. The RT current should decrease with further increase in the bias voltage and terminate when E_{ce} lines up with E_0. The observed current peaks are caused by superposition of such 3D-0D RT current components. This is an observation of tunneling phenomena through individual InAs coherent islands. Although current peaks due to tunneling through donor impurity related 0D electronic states have been reported[15-17], in our case, the observed current peaks have nothing to do with impurities because care was taken to avoid impurity diffusion or segregation, and samples B and C do not exhibit such peaks.

Moreover, as shown in Fig. 5, near the origin, we have observed charging phenomena: suppression of the current (−10-10 mV), which is considered to be due to a Coulomb blockade, and a step-like structure (−20-20 mV) considered to be a Coulomb staircase. The characteristic Coulomb energy (estimated from the onset current bias or staircase step width) is ~ 10 meV, which corresponds to a capacitance value of ~ 8 aF. Assuming a series of double tunnel capacitors, this capacitance value corresponds to a capacitance cross section of ~ 600 nm^2. This is in good agreement with the lateral size of the coherent islands measured by AFM.

4 Summary

In summary, we have fabricated GaAs/AlGaAs/InAs/AlGaAs/GaAs tunneling diodes and carried out tunneling current spectroscopy. As a result, we have observed tunneling phenomena through both 2D states in the InAs wetting layer and 0D states in the InAs coherent islands. Furthermore, we have observed Coulomb blockade of tunneling through 0D states in the InAs coherent islands. The tunneling current through 0D states and the Coulomb blockade effect are observed only for the InAs layer after formation of the coherent islands, i.e., after the growth mode transition from two-dimensional growth to three-dimensional growth. Therefore, we have shown that the difference between the InAs layers before and after the growth mode transition can be studied by tunnelling current spectroscopy.

Acknowledgements

This work was performed under the management of FED as a part of the MITI R&D program (Quantum Functional Device Project) supported by NEDO.

References

1) D. J. Eaglesham and M. Cerllo, Phys. Rev. Lett. **64**, 1943 (1990).
2) M. Tabuchi, S. Noda, and A. Sasaki in *Science and Technology of Mesoscopic Structures*, ed. S. Namba, C. Hamaguchi and T. Ando (Springer-Verlag, Tokyo, 1992).
3) D. Leonard, M. Krishnamurthy, C. M. Reaves, S. P. Denbaars, and P. M. Petroff, Appl. Phys. Lett. **63**, 3203 (1993).
4) J. M. Moison, F. Houzay, F. Barthe, L. Leprince, E. André, and O. Vatel, Appl. Phys. Lett. **64**, 196 (1994).
5) A. Madhukar, Q. Xie, P. Chen, and A. Konkar, Appl. Phys. Lett. **64**, 2727 (1994).
6) V. Bressler-Hill, A. Lorke, S. Varma, P. M. Petroff, K. Pond, and W. H. Weinberg, Phys. Rev. **B50**, 8479 (1994).
7) D. Leonard, K. Pond, and P. M. Petroff, Phys. Rev. **B50**, 11687 (1994).
8) J. Oshinowo, M Nishioka, S. Ishida, and Y. Arakawa, Appl. Phys. Lett. **65**, 1421 (1994).
9) G. Wang, S. Fafard, D. Leonard, J. E. Bowers, J. L. Merz, and P. M. Petroff, Appl. Phys. Lett. **64**, 2815 (1994).
10) S. Fafard, D. Leonard, J. L. Merz, and P. M. Petroff, Appl. Phys. Lett. **65**, 1388 (1994).
11) J.-Y. Marzin, J.-M. Gérard, A. Izabel, D. Barrier, and G. Bastard, Phys. Rev. Lett. **73**, 716 (1994).
12) M. Grundmann, J. Christen, N. N. Ledentsov, J. Böhrer, D. Bimberg, S. S. Ruvimov, P. Werner, U. Richter, U. Gösele, J. Heydenreich, V. M. Ustionv, A. Yu. Egorov, P. S. Kope'v, and Zh. I. Alferov, Phys. Rev. Lett. **74**, 4043 (1995).
13) H. Drexler, D. Leonard, W. Hansen, J. P. Kotthaus, and P. M. Petroff, Phys. Rev. Lett. **73**, 2252 (1994).
14) G. Medeiros-Ribeiro, D. Leonard, and P. M. Petroff, Appl. Phys. Lett. **66**, 1767 (1995).
15) M. W. Dellow, P. H. Beton, C. J. G. M. Langerak, T. J. Foster, P. C. Main, L. Eaves, M. Henini, S. P. Beaumont, and C. D. W. Wilkinson, Phys. Rev. Lett. **68** 1754, (1992).
16) A. K. Geim, P. C. Main, N. La Scala, Jr., L. Eaves, T. J. Foster, P. H. Beton, J. W. Sakai, F. W. Sheard, M. Henini, G. Hill, and M. A. Pate, Phys. Rev. Lett. **72** 2061, (1994).
17) A. K. Geim, T. J. Foster, A. Nogaret, N. Mori, P. J. McDonnell, N. La Scala, Jr., P. C. Main, and L. Eaves, Phys. Rev. **B50** 8074, (1994).